Molecular Properties of a Stratum Corneum Model Lipid System: Large Unilamellar Vesicles

Rita M. Hatfield*‡ and Leslie W.-M. Fung*

*Department of Chemistry, Loyola University of Chicago, Chicago, Illinois 60626, and ‡ Helene Curtis Industries, Inc., Chicago, Illinois 60639 USA

ABSTRACT Stratum corneum lipids are relatively complex, and there is little detailed understanding of their chemical and physical properties at the molecular level. Large unilamellar vesicles (LUVs) with lipid compositions similar to those of stratum corneum were prepared at pH 9 with commercially available lipids. This system was used as a model system for molecular studies of stratum corneum lipids. LUVs were chosen as the model system as they are comparatively more stable and can be characterized more quantitatively in terms of lipid concentration, surface area, and volume than model systems such as lipid mixture suspensions, lipid films, and small unilamellar vesicles. Results from freeze-fracture and cryo electron microscopy studies of our LUVs showed spherical vesicles. Quasi-elastic light scattering measurements revealed a narrow size distribution, centering around 119 nm. At room temperature, the LUVs were stable for several weeks at pH 9 and for more than 15 h but less than 24 h at pH 6. Differential scanning calorimetry measurements indicated broad endothermic transitions centered near 60–65°C, closely matching the transition temperature reported for stratum corneum lipid extracts. Spin probes, 5-doxylstearic acid and 12-doxylstearic acid, were used for electron paramagnetic resonance (EPR) studies of the molecular dynamics of the lipids. EPR results indicated more restricted motion near the polar headgroup region than near the center of the alkyl chain region. Motional profiles of the spin labels near the polar headgroup and within the alkyl chain region in the LUVs were obtained as a function of temperature, ranging from 25 to 90°C. We also found that the partitioning between the lipid and aqueous phases for each spin probe was temperature dependent and was generally correlated with phase transitions observed by differential scanning calorimetry and with alkyl chain mobility observed by EPR. Thus, this LUV system is well suited for additional molecular studies under different experimental conditions.

INTRODUCTION

The skin is a barrier for most substances entering or leaving the body, and yet selective permeability for certain molecules, including water molecules, is an essential function of skin (Scheuplein and Blank, 1971; Downing, 1992; Williams and Barry, 1992). The origin of the selective permeability of the skin, and its quantitative prediction in terms of the relevant physical and chemical properties of skin and of penetrating molecules, have been the focal point for the study of skin permeability (Scheuplein and Blank, 1971; Downing, 1992). The outermost layer of mammalian skin is the stratum corneum. The stratum corneum is composed of ~15 layers of dead cells (corneocytes) in a lipid matrix and consists of 5–15% lipids (dry weight), 75–80% proteins, and 5–10% unknown materials (Williams and Barry, 1992). Despite their overall small percentage in the stratum corneum, lipids play an important role in the selective permeability of the skin. Removal of either the entire stratum corneum or just the lipid component of the stratum corneum in the skin results in similar increases in water flux through the modified skin (Blank, 1952; Onken and Moyer, 1963). In addition, the composition and structural arrangement of stratum corneum lipids affect topical drug delivery (Hadgraft et al., 1992). The lipid composition of the stratum corneum is unusual relative to many well known biological membranes, consisting primarily of cholesterol, ceramides, free fatty acids, and cholesterol sulfate, with little phospholipids (Gray et al., 1982; Wertz et al., 1987). Although these lipids form lamellar sheets in intact stratum corneum (Elias and Friend, 1975; Madison et al., 1987), the stratum corneum membrane is believed to differ from the vast majority of mammalian cell membranes (Kitson et al., 1994). A better understanding of the molecular properties of stratum corneum lipids is critical to studies on the physiology and pathophysiology of the stratum corneum.

Many model systems have been prepared either for studies of the stratum corneum lipid properties or for studies of lipid-molecule interactions. These model systems include different dispersions of lipids in water or buffer solutions (Friberg and Osborne, 1985; White et al., 1988; Kittayanond et al., 1992; Kim et al., 1993b; Mattai et al., 1993; Kitson et al., 1994), sonicated lipid suspensions, including the preparation of small unilamellar vesicles (SUVs) (Gray and White, 1979; Wertz et al., 1986; Kittayonand et al., 1992; Blume et al., 1993; Kim et al., 1993a; Kitagawa et al., 1993), and large unilamellar vesicles (LUVs) prepared by extrusion methods (Abraham, 1992; Downing et al., 1993). We chose LUVs as the model system because LUVs were comparatively more stable than the often used but highly strained, meta-stable SUVs (Szoka, 1987). In addition, the LUV system can be characterized more quantitatively in terms of lipid concentration, surface area, and volume than multilamellar vesicle (MLV) systems, which are also quite stable. Thus the LUV

Received for publication 28 July 1994 and in final form 17 October 1994.

Address reprint requests to Dr. Leslie W.-M. Fung, Department of Chemistry, Loyola University of Chicago, 6525 N. Sheridan Rd., Chicago, IL 60626-5385. Tel.: 312-508-3128; Fax: 312-508-3086; E-mail: lfung@orion.it.luc.edu.

0006-3495/95/01/196/12 $2.00

system, with known internal volume, lipid concentration, and surface curvature, could be used, for example, in detailed molecular studies of lipid-molecule interaction or in quantitative determination of permeability and transport by stratum corneum lipids.

A variety of lipid compositions have been used in model systems. Although some investigators use phospholipids as a model of the bilayer structure of the stratum corneum (Kitson et al., 1992), most use different mixtures of ceramide, cholesterol, free fatty acid, and cholesterol sulfate. Different ceramides, including epidermal ceramide (Gray and White, 1979; White et al., 1988; Abraham, 1992; Downing et al., 1993; Kim et al., 1993a) or bovine brain ceramide type III (Kittayanond et al., 1992; Blume et al., 1993; Kitson et al., 1994), type IV (Kitagawa et al., 1993), or a mixture of bovine brain type III and IV (Mattai et al., 1993), have been used. Various fatty acids, ranging from carnauba fatty acids (used to simulate C20-C30 fatty acids, but not commercially available) (Abraham, 1992; Downing et al., 1993), to mixtures of fatty acids (Friberg and Osborne, 1985; Kim et al., 1993a; Mattai et al., 1993), to just palmitic acid (Wertz et al., 1986; Kittayanond et al., 1992; Blume et al., 1993; Kim et al., 1993b; Kitagawa et al., 1993; Kitson et al., 1994) have also been used. Thus most of the model systems are qualitatively similar but quantitatively very different. No systematic comparison of these model systems is available. In this study, we used a lipid composition that was closer to that of the native system than that used in many of the above mentioned studies. We also used lipids that were conveniently (commercially) available.

We have used both cryo- and freeze-fracture electron microscopy (EM) to observe the shape of the vesicles, quasi-elastic light scattering (QELS) to determine size distribution, differential scanning calorimetry (DSC) to obtain thermal transition temperature, and spin label electron paramagnetic resonance (EPR) techniques to monitor the molecular dynamics of lipids. Many of the physical techniques that we used have been extensively used in characterizing phospholipid vesicle systems. However, these techniques have not been applied to stratum corneum lipid systems until recently (Golden et al., 1987; Hou et al., 1991). Stability of the LUVs at different pH values was followed. We also demonstrate, by EPR techniques, how this model system can be used to study partitioning of molecules with slightly different structures (two different fatty acid derivative spin labels) resulting in very different partitioning in the stratum corneum lipid vesicles.

MATERIALS AND METHODS

All glassware was acid washed and rinsed with deionized water. Cholesterol, cholesterol sulfate, bovine brain ceramides types III and IV (containing α-hydroxy acids), lignoceric acid, and octacosanoic acid were purchased from Sigma Chemical Co. (St. Louis, MO), and palmitic acid was purchased from Fisher Scientific (Pittsburgh, PA) with at least 99% purity and used without further purification. Chemicals used to prepare the buffers were purchased from Fisher or Calbiochem (La Jolla, CA). Borate buffer from Fisher, which was labeled as 0.1 M boric acid-KCl-NaOH at pH 9 (Fisher borate buffer) was used. This buffer contained 30 mM boric acid, 70 mM KCl, and 0.2 mM EDTA (technical information from Fisher).

MLVs

The weight percentages of lipids found in the stratum corneum, 55% ceramides, 25% cholesterol, 15% free fatty acids, and 5% cholesterol sulfate (Wertz et al., 1987; Abraham, 1992), were used to prepare MLVs. In this study, we used ceramides types III and IV (3:2 weight ratio) to represent ceramides and palmitic, lignoceric, and octacosanoic acids (1:2:1 weight ratio) to represent free fatty acids. The lipids were solubilized in a chloroform and methanol mixture (2:1 volume ratio). The solvent was then removed with nitrogen gas followed by pumping under vacuum overnight to deposit a lipid thin film on a round bottom flask. Fisher borate buffer (3 ml for 15 mg total lipid) and a few glass beads were added to the lipid film, followed by hand swirling, vortexing, and heating to 70°C in a water bath to give MLVs at pH 9.

LUVs

LUVs in Fisher borate buffer were prepared from fresh MLVs by extrusion methods (Hope et al., 1985) at 70°C with a lipid extruder (Lipex, Vancouver, BC, Canada). The lipid concentrations in MLVs were usually ~5 mg/ml, but higher concentrations, up to 20 mg/ml, were also used. The MLVs were subjected to five freeze-thaw cycles before extrusion (Mayer et al., 1985). Polycarbonate filters (Costar Nucleopore, Cambridge, MA) with 5-, 1-, 0.4-, and 0.1-μm pore sizes were used in the extruder in the order listed (Abraham, 1992) to give stable LUVs at pH 9.

Buffers at different pH values were prepared with osmolality values matching the value of Fisher borate buffer (150 ± 10 mmol/kg), measured with a vapor pressure 5500 osmometer (Westcor, Logan, UT). A borate solution (7.5 mM sodium tetraborate, 60 mM KCl, 0.2 mM EDTA) was prepared and titrated with concentrated HCl to either pH 7.4 or 6.0. Sodium phosphate (72 mM) buffer at pH 7.4 was also prepared.

To better compare the properties of LUVs at different pH values, LUVs at 10 mg/ml were prepared and diluted to ~1 mg/ml with Fisher borate buffer at pH 9. Different portions (generally 2 ml) of the batch were dialyzed with different buffers (borate at pH 7.4 or 6 or phosphate buffer at pH 7.4) at 500-fold excess volume. The pH of the LUV solution inside the dialysis tubing (14K MWCO from Spectrum Medical Industries, Houston, TX) was checked, and it was found that ~3 h were needed for pH equilibration with borate solution and ~1 h with phosphate buffer. The pH values of all LUV samples (~1 mg/ml) were measured periodically after dialysis for 24 h. We also measured the pH of LUV samples after the samples were subjected to freeze-thaw cycles immediately after dialysis.

Lipid composition determination

The lipids in the vesicle suspensions were extracted by chloroform, methanol, and water (1:1:1 volume ratio). Potassium chloride (0.1 M) was added to insure that all cholesterol sulfate was recovered in the chloroform phase (Williams and Elias, 1981). Additional potassium chloride was added, if necessary, to help separate the phases. The lipid compositions in the chloroform extracts of MLVs and LUVs were determined by high performance thin layer chromatography (HPTLC) on silica gel 60 plates (E. M. Separations, Gibbstown, NJ). The plates (10 × 20 cm) were developed, charred (Melnik et al., 1989), and scanned with a TLC scanner II (CAMAG, Muttenz, Switzerland) interfaced to a CR3A Cromatopac integrator (Shimatzu Corp., Kyoto, Japan). The peak area of each spot in a MLV sample was correlated with the known mass of the corresponding lipid in MLVs. This mass over peak area ratio was then used to convert the peak area of the corresponding LUV lipid spot to lipid mass. This conversion process was necessary because the lipids used did not char to the same extent to give the same linear relationship between spot intensities and masses for all lipids. The total mass of all the lipids in the LUV sample was obtained from the sum of individual lipid masses. The value of this sum divided by

the total MLV lipid mass represented the recovery of lipid after extrusion. The LUV lipid composition was then determined from the values of individual and total masses in the LUV sample.

Vesicle size

Freeze-fracture and cryo-EM were performed by Northern Lipids Inc. (Vancouver, BC, Canada), as a service, on LUVs (20 mg/ml) in Fisher borate buffer at pH 9.

Photon correlation spectroscopy of QELS measurements with a particle size analyzer (BI 90; Brookhaven Instruments, New Haven, CT) was used to determine the hydrodynamic effective diameters of the LUVs in different buffer systems. Immediately after dialysis, LUV samples (5–10 mg/ml) were diluted 2- to 10-fold as necessary to bring the photon count rate within the recommended range (250–500 kcps) for vesicles with effective diameters of 100–300 nm. At least two different lipid concentrations were used for each sample to show that the diffusion coefficient of the sample did not change on dilution. Typically 7500 cycles (6.25 min) were used. The dust cutoff for the instrument was kept constant for all samples. If the dust factor in a sample was >0.02, the measurements were rejected. For QELS measurements carried out continuously over 24 h, the LUVs in the cuvette were kept at 25°C in the instrument throughout the entire measurement period. The sampling time was 25 min (30,000 cycles). Cumulant analysis was applied to scattering data to give effective diameters and polydispersity. If the polydispersity of a LUV sample was >0.11, the QELS measurements of this sample were not used, and the sample was also not used for preparing LUVs at different pH values. To further determine whether the diameter distribution was a broad unimodal or a skewed, multimodal distribution, inverse Laplace transform analysis, with an exponential sampling technique, was also used. This analysis, however, gave a less rigorous analysis of the particle size. Thus we used the effective diameter from cumulant analysis as the size of the samples.

DSC

Lipid thin films, similar to those used for MLVs, were scraped from the walls of a round bottom flask and sealed in an aluminum sample pan. The sample (3–4 mg) was then equilibrated to 5°C in a differential scanning calorimeter (DSC 2910; Thermal Analysis Instruments, New Castle, DE). The sample was initially heated from 5 to 90°C at a rate of 2°C/min and then cooled back to 5°C at the same rate. Heat flow (thermogram) was then recorded during the second heating process. Thermograms were also obtained during the third cooling and heating processes to determine whether the observed thermal transitions were reversible. Most samples were used immediately after they were transferred to sealed sample pans. Some samples remained in the sealed pans for a longer period of time but less than 24 h. No differences in the second heating thermograms were observed in samples used.

Spin-labeled LUVs

Two fatty acid spin probes, 5- and 12-doxylstearic acid (5- and 12-DSA) were purchased from Molecular Probes (Eugene, OR) or Syva (Palo Alto, CA) and used without further purification. 5-DSA or 12-DSA in ethanol was dried to a thin film with a gentle stream of nitrogen gas. A sample of LUVs at pH 9 was then added to the spin label thin film at a lipid-to-spin label molar ratio of ~150 to avoid spin-spin exchange (Fung and Johnson, 1984). The spin label concentrations in samples were generally $\sim 7 \times 10^{-5}$ to 8×10^{-5} M. The spin label was also directly incorporated into the lipid thin film by adding the spin label in ethanol to the lipids in chloroform-methanol before nitrogen gas evaporation. No significant spectral differences were found by the two different labeling methods. Samples of spin labels in borate buffer ($\sim 2 \times 10^{-5}$ M) were used as controls and were prepared in tandem with the spin-labeled LUV samples.

EPR measurements

EPR measurements were performed by using a Varian E-109 EPR spectrometer equipped with an IBM variable temperature control unit (Fung and Zhang, 1990). One gauss modulation, 60-s scan time, and 5-mW microwave power were used to obtain EPR spectra. The EPR cavity with a standard quartz EPR tube filled with silicone fluid to provide thermal stability was prewarmed to a desired temperature, which was monitored by a copper-constantan thermocouple (Fung and Zhang, 1990). The spin-labeled LUV sample was placed in the cavity for 2 min before data acquisition to assure thermal equilibration. After each EPR measurement, the sample was removed from the cavity and placed in a water bath at the same temperature until the cavity reached a new temperature equilibrium. Temperatures from 25 to 90°C were used.

EPR data analysis

Spectral subtraction

Spectral subtraction, with commercially available software ASYST (MacMillan Software, New York, NY.), modified for EPR operation, was performed to deconvolute the fast (weakly immobilized) and slow (strongly immobilized) components in spin-labeled LUV spectra (Fig. 1*A*). We were able to use the spectra of spin labels in buffer at matching temperatures (Fig. 1*B*) to remove the weakly immobilized component in the spectra of labeled LUVs at all temperatures studied to give the spectra of the slow component (Fig. 1*C*). A second subtraction provided the spectra of the fast

FIGURE 1 Typical EPR spectra at 77°C of (*A*) 5-DSA in LUVs in Fisher borate buffer at pH 9 with a lipid-to-spin label molar ratio of 150 and a spin label concentration of $\sim 4 \times 10^{-5}$ M and (*B*) 5-DSA dispersed in the same buffer. The weakly immobilized component in *A* was removed by spectral subtraction of $A - B$ to give the spectrum of spin label fraction that was intercalated in the lipid phase of LUVs (*C*).

component. This spectral subtraction procedure allowed us to use the composite spectra of LUVs to provide pairs of two single-component deconvoluted spectra for more vigorous analysis of spectral parameters, such as the intensity/concentration of each component in the LUV samples.

Spin label intensity

Spectra of a spin label in buffer at different temperatures were obtained, and results of double integration of the spectra were used to provide calibration curves for spin label intensity at different temperatures. Such procedures were required to account for differences in signal intensity due to dielectric-induced changes in cavity sensitivity at different temperatures (Fung and Johnson, 1983). For 5-DSA intensity measurements, the peak height of the central line of the weakly immobilized component was also used to estimate concentration as some samples exhibited low signal-to-noise ratio of the weakly immobilized component signal yielding unreliable double integration results.

Hyperfine splitting

The hyperfine splittings ($2A_{max}$) of the strongly immobilized component in LUV spectra were measured as the distance between the outermost EPR lines (Griffith and Jost, 1976).

Rotational correlation time

The rotational correlation times for the weakly immobilized signal in LUVs and for the strongly immobilized signal for 12-DSA in LUVs at 90°C were estimated from line width and line height measurements by using the linear terms of the motional narrowing theory (Fung and Johnson, 1984). Approximate axial correlation times (τ_R^z) for the remaining strongly immobilized signals were obtained from the following expression, which includes the temperature dependence of the hyperfine separation measurements (Johnson, 1979):

$$(\tau_R^z)^{-1} = a_z(T)[1 - A_{zz}^*/A_{zz}^o(T)]^{p_z} \quad (1)$$

For simplicity, we used this equation to estimate the rotational correlation times. Due to anisotropic averaging, more quantitative calculations of the rotational correlation times should be obtained with the spectral simulation methods provided by Freed (1976).

Partition ratio

The partitioning of fatty acid spin labels in aqueous and lipid phases in LUV samples was followed as a function of temperature. The fraction of spin labels in the aqueous phase of LUV samples ($f_{aqueous}$) at a particular temperature was obtained from the spin label intensities of deconvoluted spectra of the weakly immobilized signal, and the fraction of spin labels in the lipid phase (f_{lipid}) was obtained from the corresponding spectra of the strongly immobilized signal. The ratios of these two fractions ($f_{lipid}/f_{aqueous}$) at a particular temperature were calculated. This ratio is directly related to the partition coefficient, partial specific volume of lipid, and lipid concentration (Miyazaki et al., 1992).

RESULTS

Lipid composition, vesicle size, and stability of LUVs at pH 9

The lipid composition found in the stratum corneum (Wertz et al., 1987) was used to prepare MLVs. The HPTLC results of MLV and LUV lipids (Fig. 2) were very similar. The two spots at the top of the plate were assigned to free fatty acids (octacosanoic, lignoceric, and palmitic acids), followed by

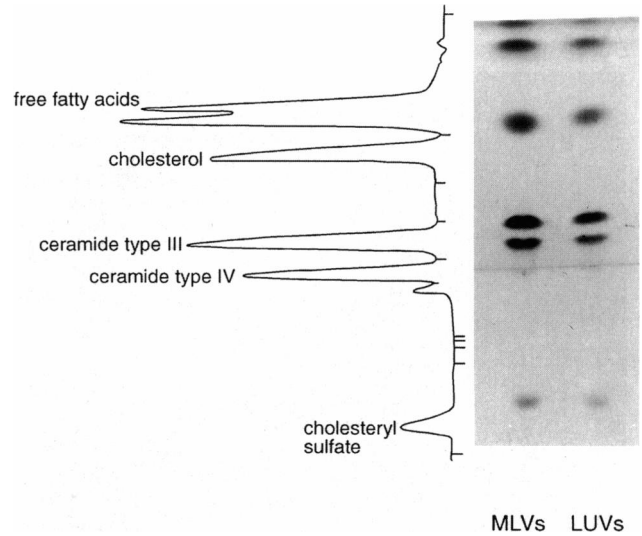

FIGURE 2 HPTLC of stratum corneum lipids in MLVs and LUVs with 50 μg total lipid for each sample. The silica gel 60 plate was first developed with chloroform:methanol:water (95:20:1 by volume) to 6.5 cm above the origin and then with hexane:diethyl ether:acetic acid (80:20:10 by volume) to ~12 cm above the origin. The plate was sprayed with 10% (w/v) cupric sulfate hydrate in 8% (w/v) phosphoric acid and charred at 170°C for 60 min for visualization. The densitometric scan of the MLV lane is shown on the left. The peak positions are not matched to the spot positions on the plate due to limited selection on chart speed used for the densitometer. The identification of each lipid spot was made with similar chromatograms of known lipid and is shown.

cholesterol, ceramide type III, ceramide type IV, and cholesterol sulfate. Scanning densitometry scans on the charred spots from three separate preparations showed 80–95% recovery of the MLV lipids in the LUV samples. Thus, the LUV preparation procedures described above gave relatively high yields of LUVs. In addition, the lipid compositions of MLVs and of LUVs (Table 1) were nearly the same. Little detectable lipid degradation or loss of specific lipid occurred as a result of either the heating or the extrusion process used in sample preparation. Thus the lipid composition of LUVs was very similar to the one designated to represent stratum corneum lipid composition.

The micrographs of LUVs at pH 9 using either freeze-fracture EM (Fig. 3*A*) or cryo-EM (Fig. 3*B*) demonstrated,

TABLE 1 Lipid composition (weight %) in MLVs and in extruded LUVs

Lipid type	MLV (%)	LUV (%)
Free fatty acid	15*	15.5 ± 1.7‡
Cholesterol	25	25.5 ± 1.9
Ceramide III	33	33.2 ± 1.0
Ceramide IV	22	20.9 ± 0.9
Cholesterol sulfate	5	5.0 ± 1.2
Total	100	101

*14 μg of total lipid were used in two runs and 25 μg in the third run.
‡ Average weight percent of three different runs. The intensities of the spots on the HPTLC plate, as shown in Fig. 2, were converted to weight percent for each lipid type, with MLV spot intensities as reference. See text for details.

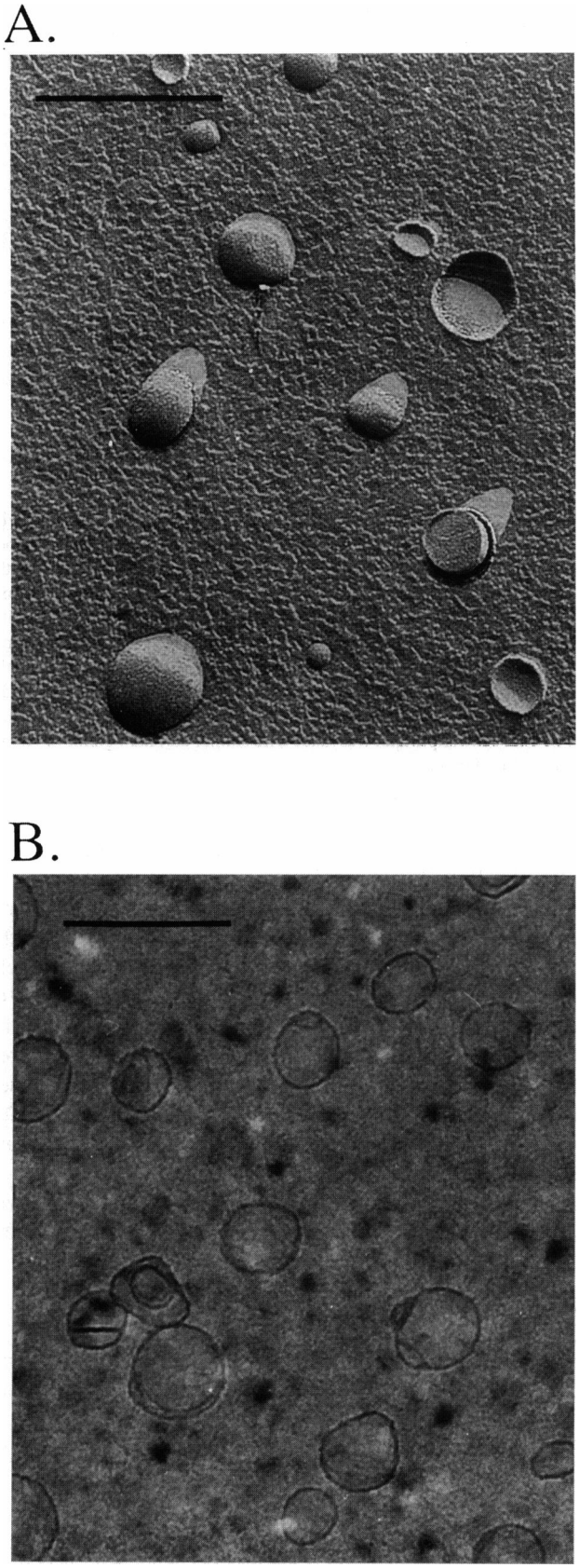

FIGURE 3 (*A*) Freeze-fracture and (*B*) cryo-EMs of LUVs at 20 mg/ml in Fisher borate buffer. The scale bars are 200 nm. The vesicles are generally spherical with a diameter of ~100 nm. The micrographs were prepared, as a service, by Northern Lipids Inc. (Vancouver, Canada).

independently, that the LUVs were predominantly spherical with average diameters of ~100 nm. Some of the vesicles also displayed an angular profile by both EM techniques, which has been observed in the presence of long, saturated acyl chains of phospholipid vesicles (Klösgen and Helfrich, 1993; T. Madden, Northern Lipids Inc., personal communication). There was a tendency for the vesicles to aggregate at the high lipid concentrations (20 mg/ml) used for EM measurements.

The average effective diameter from cumulant analysis of QELS measurements of LUVs obtained from 16 separate LUV preparations, including the 4 different preparations shown in Table 2, was 119 ± 10 nm with a polydispersity of 0.086 ± 0.019. The standard deviation of 10 nm reported with the average effective diameter was mostly due to slightly different diameters of LUVs obtained from different LUV preparations. The standard deviation of multiple QELS measurements on a single LUV sample was ≤1 nm. Because the majority of the vesicles in micrographs appeared spherical, the effective diameters obtained from cumulant analysis should be fairly accurate, as the analysis assumed particles to be spheres. Polydispersity values provided information on the relative width of the diameter distribution. Samples with values <0.08 were considered to have diameters narrowly distributed. Thus, both EM and QELS data showed that the LUVs at pH 9 had shapes similar to spheres with diameters rather narrowly distributed around 100–120 nm. These LUVs were also quite stable upon storage at room temperature. The average effective diameter of LUVs after 48 h of storage remained at ~114 nm with a polydispersity of 0.076. Inverse Laplace transform analysis showed a single population of LUVs with a diameter centered around 116 nm for the time studied. Thus, the effective diameters of LUVs remained narrowly centered around 114 nm after 48 h of storage at room temperature. The LUV samples (1 mg/ml) remained free of precipitation for 4–6 weeks, suggesting that these vesicles were very stable at room temperature.

Effect of pH on vesicle effective diameter and polydispersity

Upon decreasing the pH values of LUV samples, the average effective diameter of LUVs in borate solution increased slightly, from 114 nm at pH 9 to 117 nm at pH 7.4 and 128 nm at pH 6.0 (Table 2, top panel). The corresponding values for polydispersity increased from 0.091 to 0.137 and 0.177, respectively. Size distribution results from inverse Laplace transform analysis also indicated more than one population. The average diameter in each population exhibited large standard deviations and the intensity-weighted percentages also varied greatly from run to run, suggesting that the size of LUVs in borate buffer at pH 7.4 and 6.0 was somewhat heterogeneous and varied from run to run. Upon storage for 48 h, the LUVs in borate at pH 7.4 further increased their size (127 nm) and heterogeneity (polydispersity = 0.165; Table 2, bottom panel). For LUVs at pH 6.0, storage for 48 h rendered samples with precipitation. Consequently, large dust

TABLE 2 QELS particle size analysis (by both cumulant and inverse Laplace transform analysis methods) of LUVs in borate buffer at different pH values and in phosphate buffer at pH 7.4, with measurements taken immediately after dialysis (top panel) and 48 h later (bottom panel)

				Inverse Laplace transform analysis			
		Cumulant analysis		Population 1[c]		Population 2	
Buffer	pH	ED[a] (*n*)	PD[b] (*n*)	D[d] (*n*)	Fraction (%)[e]	D (*n*)	Fraction (%)
Borate	9.0	114 ± 13 (4)	0.091 ± 0.014 (4)	116 ± 13 (4)	100	ND[f]	ND
Borate	7.4	117 ± 11 (4)	0.137 ± 0.035 (4)	97 ± 26 (4)	32–100	226 ± 121 (3)	0–68
Borate	6.0	128 ± 16 (5)	0.177 ± 0.053 (3)	112 ± 23 (5)	44–100	333 ± 171 (3)	0–56
Phosphate	7.4	133 ± 23 (3)	0.184 ± 0.042 (3)	128 ± 16 (3)	100	ND	ND
Borate	9.0	114 ± 13 (3)	0.076 ± 0.005 (3)	119 ± 16 (3)	100	ND	ND
Borate	7.4	127 ± 11 (4)	0.165 ± 0.047 (4)	120 ± 15 (4)	76–100	796 ± 100 (2)	0–24
Borate	6.0	NA[g]	NA	NA	NA	NA	NA
Phosphate	7.4	140 ± 13 (3)	0.192 ± 0.042 (3)	116 ± 9 (3)	74–82	592 ± 241 (3)	18–26

[a] ED, average effective diameter in nanometers of LUV ± SD (*n*, number of different samples used).
[b] PD, polydispersity (the relative width of the distribution of ED).
[c] Populations 1 and 2 represent the two subpopulations identified by the inverse Laplace transformation analysis.
[d] D, center diameter (in nanometers) for each subpopulation ± SD deviation (*n*, number of samples with the subpopulation).
[e] Fraction is the intensity-weighted fraction. The value (%) is shown as a range of values obtained from all samples. For example, for LUVs in borate buffer at pH 7.4, in population 1, the percents for D = 93, 75, 134, and 86 nm were 73, 32, 100, and 42%, respectively, and the corresponding percents in population 2 with D = 366, 146, and 168 nm were 27, 68, and 58%, respectively.
[f] ND, not detected.
[g] NA, not analyzed, due to large amounts of precipitation (large dust factors) in the sample (see Fig. 4).

factors were obtained for QELS measurements and the data were not analyzed. HPTLC analysis of the precipitated lipid showed the presence of all lipids, suggesting that the LUVs had fallen apart at pH 6.0 after storage at room temperature for 48 h.

We have also followed a LUV sample at pH 6.0 immediately after preparation with QELS for ~18 h continuously. As shown in Fig. 4, the effective diameters increased gradually over 15 h, from 112 to ~119 nm. The corresponding polydispersity values also increased from 0.145 to 0.196. The dust factors in the sample remained ~0.01, indicating that the sample was still relatively dustfree. After 15 h, the dust factor increased suddenly to ~0.07 at 16 h and 0.12 at 17 h. The effective diameters and polydispersity values both dropped, signifying an onset of drastic changes in the LUV sample, which led to the eventual precipitation of LUVs, as shown in samples after storage for 48 h (Table 2, bottom panel). As shown in Fig. 4, QELS properties of the control sample (LUVs at pH 9) remained essentially the same throughout the time period studied.

Because borate buffer has little buffering capacity at pH 7.4 and 6.0, we also dialyzed the pH 9 LUV samples with phosphate buffer at pH 7.4. The effective diameters of LUVs in phosphate buffer were ~15 nm larger than those in borate solution at pH 7.4 (Table 2, top panel). The polydispersity values increased from 0.137 to 0.184. Inverse Laplace transform analysis showed one population with an average diameter of 128 nm, in good agreement with results obtained from the cumulant analysis. Thus the LUVs in phosphate buffer at pH 7.4 appeared to have diameters broadly distributed around 130 nm. Upon storage for 48 h, the effective diameters appeared to increase slightly to ~140 nm. Inverse Laplace transform analysis revealed two populations of different diameters in the LUV samples, with the majority centered around 120 nm and a minor group centered around 600 nm (Table 2, bottom panel). These data suggested that the LUVs in phosphate buffer at pH 7.4 were ~10–15 nm larger than those at pH 9 and were not as stable as the LUVs at pH 9.

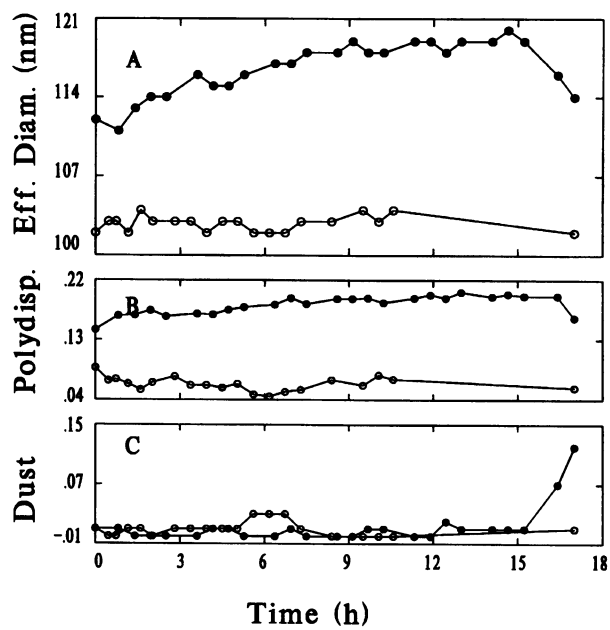

FIGURE 4 QELS particle size analysis. (*A*) Effective diameter, (*B*) polydispersity, and (*C*) dust factor, of LUVs prepared in Fisher borate buffer at pH 9 (○) and then dialyzed in 7.5 mM borate buffer containing 60 mM KCl and 0.2 mM EDTA at pH 6 (●) as a function of time. The osmolarity of the buffers was 150 ± 10 mOsm. QELS measurements were continuously recorded until the dust factor increased significantly. The total lipid concentration of the sample was approximately 1.3 mg/ml. The sample was kept under atmospheric pressure at 25°C during measurement. Time zero represents the time when the contents inside the dialysis tubing reached pH 6.

It should be noted that, when the LUVs in borate buffer at pH 9 were subjected to dialysis to pH 7.4 or 6.0 according to the procedures that we used, the external pH of the LUVs reached the designated pH value. The internal pH values of the LUVs were not necessarily the same as the external pH values. Previous studies of phospholipid vesicles prepared in borate buffer at pH 10.5 and injected into HEPES buffer at pH 7.4 have shown the existence of a pH gradient of ~3 units across the vesicle bilayer for at least 30 min (Wilschut et al., 1992). It has also been found that borate does not readily permeate phospholipid vesicles (Eastman et al., 1989). We performed simple pH measurements on our LUV samples at pH 7.4 in both phosphate and borate buffers. Whereas a 0.05 pH unit increase was noted for LUVs in borate at pH 7.4, no detectable change in pH was observed for LUVs in phosphate buffer. For LUVs at pH 6.0, a 0.40 pH unit increase was measured. Changes similar in pH to those described above were also measured for LUV samples subjected to freeze-thaw cycles immediately after dialysis. The buffers and solutions themselves showed no increases in pH over time. No detectable changes in pH were measured for samples of LUVs at pH 9. It is likely that stratum corneum lipid bilayers also exhibit pH gradients similar to those observed in phospholipid bilayers. More detailed studies are needed for a better understanding of the pH properties of stratum corneum LUVs prepared at pH 9 and dialyzed to pH 7.4 or 6.0.

Thermal properties of lipid mixtures of LUVs

Second heating thermograms of stratum corneum lipid mixtures with a lipid composition used for LUV preparation showed two broad, enthalpic transitions centered at ~60°C and at 65°C, with a shoulder at ~70°C (Fig. 5). These transitions were also detected in the third heating thermogram, indicating that the enthalpic transitions were reversible. First heating thermograms of some samples exhibited only one broad transition instead of a doublet with variations in the temperature at which the transition was centered (56–65°C). These slight differences could be due to variations in sample preparations, including moisture contents in lipids. Regardless of the variation observed in the thermograms of first heating, the thermograms of the second and third heating were essentially the same.

Phase transitions for stratum corneum are complex and have been studied by x-ray diffraction, infrared spectroscopy, and DSC techniques. DSC results reported transitions at 35, 65, and 80°C for intact human stratum corneum and at 60 and 70°C for porcine stratum corneum (Golden et al., 1986; 1987). DSC studies of lipid extracts show a broad lipid transition at 60°C for porcine stratum corneum (Golden et al., 1987) and at 65°C for human stratum corneum (Golden et al., 1986). These transitions have been attributed to alkyl chain melting. Our results were in good agreement with published results.

Dynamic properties of lipids in LUVs

The EPR spectra of LUVs labeled with 5-DSA or 12-DSA at pH 9 showed a composite spectra of weakly and strongly immobilized components at all temperatures. Typical spectra of 5-DSA and 12-DSA in LUVs at 25 and 90°C are shown in Fig. 6. As indicated in Materials and Methods, the weakly immobilized component spectra of either 5-DSA- or 12-DSA-labeled LUV samples at a specific temperature were identical to spectra of 5-DSA or 12-DSA, respectively, in buffer at the same temperature. At 25°C, the rotational correlation time obtained from the spectrum of the spin label in aqueous environment was approximately 1.3×10^{-10} s for 5-DSA and 1.5×10^{-10} s for 12-DSA. At 90°C, the apparent correlation time was 3.8×10^{-11} s for 5-DSA and 3.7×10^{-11} s for 12-DSA. These rotational correlation time results were in good agreement with published values for doxylstearic acid spin labels dispersed in buffer (Brown et al., 1981). Thus these spectra provided evidence that the fatty acid derivative

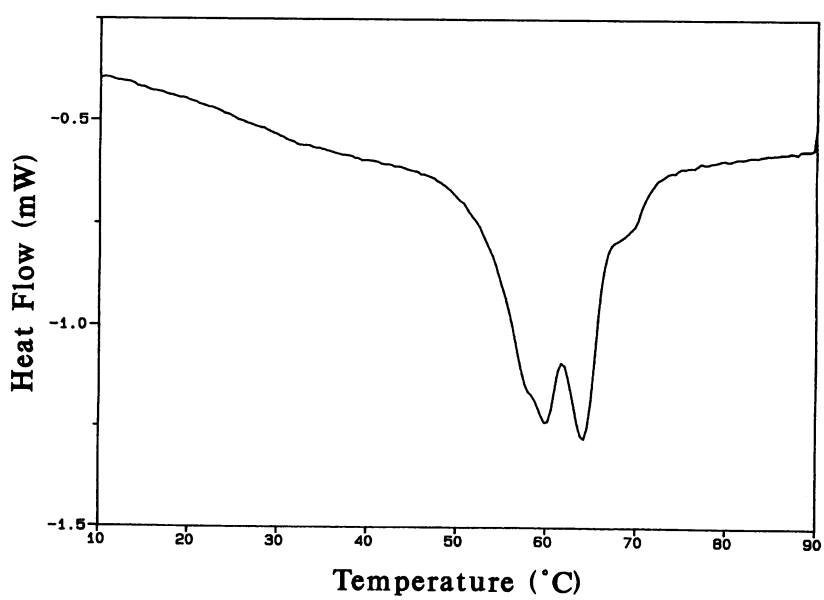

FIGURE 5 DSC thermogram of a typical stratum corneum lipid thin film prepared with a lipid composition the same as that used to prepare LUVs. The thermogram represents the second reheat of the sample at a scan rate of 2°C/min. The film was evacuated under vacuum pressure and stored in a closed container until use. Transitions at ~60 and 65°C were observed.

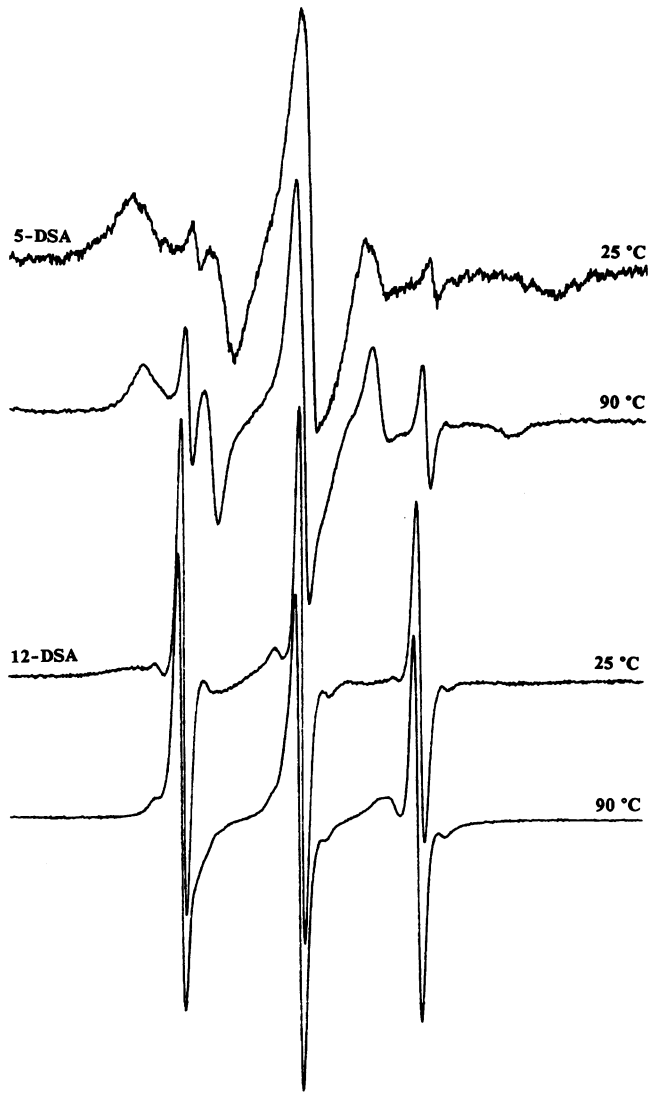

FIGURE 6 Selected EPR spectra of 5-DSA and 12-DSA in LUVs in Fisher borate buffer at pH 9. A lipid-to-spin label molar ratio of 150 with a spin label concentration of 7.5×10^{-5} M was used. Different spin label partitions in the LUV bilayer and aqueous phases to give different intensities of broad (lipid-like) and sharp (aqueous-like) signals are seen in these spectra at 25 and 90°C.

spin labels partitioned into the aqueous phase as well as into the lipid phase in LUVs.

The strongly immobilized EPR signals were those of 5-DSA and 12-DSA intercalated into the lipid bilayer producing relatively slow motion. A typical spectrum, from spectral subtraction, of the strongly immobilized (lipid) component of 5-DSA in LUVs at 77°C is shown in Fig. 1*C*. The $2A_{max}$ of the lipid component is proportional to label mobility (Griffith et al., 1974). $2A_{max}$ has been used as an empirical measure of mobility of lipid molecules (Marsh, 1982). The $2A_{max}$ of strongly immobilized 5-DSA signals in LUVs at 25°C was 55.4 ± 1.1 G (n = 3). The corresponding apparent rotational correlation time was $\sim 1.2 \times 10^{-8}$ s. The $2A_{max}$ of 12-DSA in LUVs at 25°C was 54.1 ± 3.3 G, with a corresponding apparent rotational correlation time of $\sim 9.8 \times 10^{-9}$ s. As the temperature of the samples increased, $2A_{max}$ decreased, as expected, for both fatty acid spin labels. However, the quantitative effects of temperature on $2A_{max}$ were different for the two probes. The $2A_{max}$ values of 12-DSA (Fig. 7*B*) decrease much faster than those of 5-DSA (Fig. 7*A*) upon temperature increase. At 90°C, $2A_{max}$ was 48.9 ± 0.6 G for 5-DSA, corresponding to a rotational correlation time of $\sim 5.1 \times 10^{-9}$ s, but was 34.2 ± 1.1 G for 12-DSA, corresponding to $\sim 1.2 \times 10^{-9}$ s. For 5-DSA, $2A_{max}$ was inversely proportional to temperature and exhibited a rather linear behavior between 25 and 90°C. However, for 12-DSA, a gradual, but not linear, decrease in $2A_{max}$ was observed from 25 to 72°C. The largest change in $2A_{max}$ was observed at ~60°C. Above 72°C, little change was observed in $2A_{max}$.

Partitioning of fatty acid spin labels in LUVs

Inasmuch as we have demonstrated that both 5-DSA and 12-DSA molecules partition between lipid and aqueous phases, the intensity ratios of the spin labels in the lipid and aqueous phases provided quantitative information on the partitioning in stratum corneum LUVs. When 5-DSA and 12-DSA were introduced to LUVs at pH 9 and 25°C at a lipid-to-spin label ratio of 150, only ~1.0 ± 0.1% (n = 3) of 5-DSA but ~26.0 ± 5.8% (n = 2) of 12-DSA were in the aqueous phase. At 90°C, ~4.5 ± 1.2% of 5-DSA and ~26.3 ± 7.2% of 12-DSA were in the aqueous phase. The partition ratio ($f_{lipid}/f_{aqueous}$) was then 96.1 ± 3.8 for 5-DSA and only 2.9 ± 0.9 for 12-DSA at 25°C. At 90°C, the ratio decreased to 22.6 ± 5.7 for 5-DSA, whereas the ratio appeared to remain constant for 12-DSA (3.0 ± 1.1).

A careful study of the ratios as a function of temperature revealed interesting results. As shown in Fig. 8*A*, the average partition ratio ($f_{lipid}/f_{aqueous}$) for 5-DSA decreased sharply,

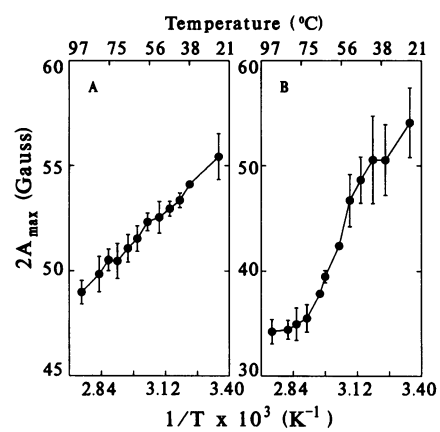

FIGURE 7 The hyperfine splitting of the strongly immobilized component ($2A_{max}$) from the spectra of (*A*) 5-DSA (n = 3) and (*B*) 12-DSA (n = 2) in LUVs in Fisher borate buffer at pH 9. A lipid-to-spin label molar ratio of 150 with a lipid concentration of 5 mg/ml was used. Note that vertical scales for the two plots differ because the two spin labels exhibit different $2A_{max}$ values. The temperature values given on the top of the plots are rounded off and are not necessarily precise. Data are presented by using the bottom inverse temperature scale.

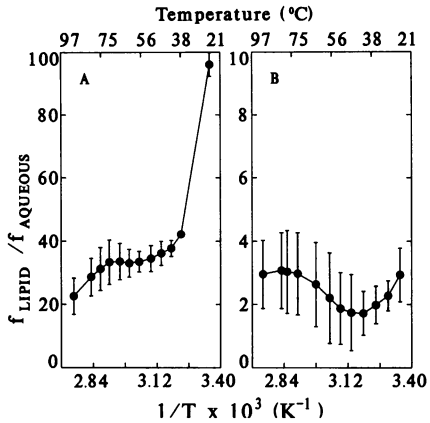

FIGURE 8 The average partition ratio ($f_{lipid}/f_{aqueous}$)) of (*A*) 5-DSA (n = 3) and (*B*) 12-DSA (n = 2) in LUVs in Fisher borate buffer at pH 9 as a function of temperature. f_{lipid} values were determined from the strongly immobilized component and $f_{aqueous}$ values from the weakly immobilized component. A lipid-to-spin label molar ratio of 150 with lipid concentration of 5 mg/ml was used. Spin label intensity calibration curves were used to determine spin label intensities at different temperatures. Such procedures were required to account for the different EPR cavity sensitivity at different temperatures. Note that vertical scales for the two plots are different due to large differences in partition values of the two spin labels. The temperature values given on the top of the plots are rounded off and are not necessarily precise. Data are presented by using the bottom inverse temperature scale.

from ~96 at 25°C to ~42 at 37°C and then to ~38 at 41°C. The ratio changed only slightly from 41 to 50°C, to a value of ~35 at 50°C. Further increase in temperature in the range of 55–70°C resulted in little change in the ratio values. Above 70°C, the average ratio appeared to show a linear relationship with inverse temperature, resulting in a $f_{lipid}/f_{aqueous}$ of ~23 at 90°C.

The partition ratio versus temperature plot for 12-DSA (Fig. 8*B*) was quite different from that for 5-DSA in the same LUV system at pH 9. The partition ratios decreased slightly as the temperature was increased from 25 to 40°C and reached a minimum value of ~2 at 40–45°C. Further increase in temperature resulted in slight increase in the partition ratio to ~3 at 70°C. The ratio remained constant as the temperature was further increased to 90°C. The results presented in Fig. 8*B* were average values of two runs. The ratios of one run were consistently higher (3.5 at 25°C, for example) than those in the other run (2.3 at 25°C) by about a constant amount throughout the temperature range studied, with the minimum ~40–45°C (2.2 for the run with higher values and 0.9 for the run with lower values). Thus the temperature-induced changes in the partition coefficients for 12-DSA in LUVs were very reproducible from run to run, despite the magnitudes of the changes being quite small (maximal changes were ~1.5).

DISCUSSION

We have described detailed procedures for using lipids that are commercially available to prepare stratum corneum LUVs at pH 9 by extrusion methods. A model system consisting of conveniently available lipid components will presumably generate more studies of the system, leading to a better understanding of stratum corneum lipids on a molecular level. The experimentally determined lipid composition in LUVs was ~33% (by weight) ceramide III, 25% cholesterol, 21% ceramide IV, 16% total free fatty acids, and 5% cholesterol sulfate, a lipid composition very similar to that of the mammalian stratum corneum. Our LUV system, which is one of a few model systems that use commercially available lipids to include both ceramide types III and IV, simulates the presence of both α-hydroxy- and non-α-hydroxy-containing ceramides in the stratum corneum. We also used a combination of commercially available C16 palmitic, C20 lignoceric, and C28 octacosanoic acids to give a mixture of fatty acids with C16 to C28 chain lengths, to closely simulate the free fatty acid composition in the stratum corneum (Wertz et al., 1987). Thus we believe that the combination of the lipids that we used represent a lipid composition very similar to that in stratum corneum. Our data showed that our LUVs had a relatively uniform size distribution of ~100–120 nm at pH 9 in borate buffer with an osmolality of ~150 mmol/kg. They were stable at room temperature for at least 4–6 weeks. Our DSC data were in good agreement with published results on lipids extracted from the stratum corneum, indicating that the lipids in our LUV system were thermodynamically very similar to lipids in intact stratum corneum. Thus the advantages of our model system are that (1), lipids are easily available; (2), lipids resemble those in the stratum corneum, both in composition and in thermodynamic properties; and (3), it is a stable system with well characterized properties and thus is well suited for studies of stratum corneum lipid properties under different experimental conditions.

Many phospholipid liposomes have been used as artificial drug carriers (Lasic, 1992). The requirements for clinical application include (1), a very narrow size distribution and (2), long-term stability (Winterhalter and Lasic, 1993). Our LUV system satisfies both of these requirements and thus may be suited for further development as carriers for drug or cosmetic delivery.

Because the surface pH of the skin is ~5.5 (Behrendt and Green, 1971; Braun-Falco and Korting, 1986), model systems that can be used at different pH values will be useful. Many of the MLV, SUV, or lipid dispersion model systems were prepared at neutral or acidic pH (Friberg and Osborne, 1985; Wertz et al., 1986; Kittayanond et al., 1992; Blume et al., 1993; Kim et al., 1993b; Kitagawa et al., 1993; Mattai et al., 1993). However, these systems cannot be characterized as well as LUV systems for quantitative studies. LUVs with cholesterol sulfate and fatty acids in compositions similar to those found in stratum corneum were all prepared at pH 8.5 or above (Abraham, 1992; Downing et al., 1993) and are reportedly stable for several weeks. Cholesterol sulfate and/or free fatty acids are needed for lipid systems containing ceramides and cholesterol to form vesicles (Wertz et al., 1986; Kittayanond et al., 1992). The effective pK_a of cholesterol sulfate in membranes is <4 (Bleau et al., 1974; Kitson

et al., 1992). The apparent pK_a of fatty acid in membranes is ~7.2–7.4 (Ptak et al., 1980). Thus cholesterol sulfate and free fatty acids are completely ionized at pH 9. It appears that these charged forms of cholesterol sulfate and fatty acids are required to form stable vesicles with the lipid composition that we used. In these nonphospholipid, stratum corneum lipid vesicle systems, the precise lipid composition and the pH of the aqueous environment appear to be critical to the type of vesicle formed and its stability. In fact, recent ^2H nuclear magnetic resonance studies report that lipid compositions and pH affect the phase behavior of dispersions containing ceramide and palmitic acid and, in combination with cholesterol, phase coexistence is common over the temperature range 20–75°C (Kitson et al., 1994).

As the external pH of the LUVs at pH 9 was lowered to 7.4 and to 6.0 through dialysis, we observed small, gradual increases in effective diameter and polydispersity, leading to unstable vesicles. As the osmolality of the buffers at different pH values was the same, the observed changes were attributed to pH changes in the samples. It has been noted that borate does not readily permeate vesicle bilayers (Hope and Cullis, 1987). A pH gradient across the bilayer is maintained resulting in lipid asymmetry in vesicles containing phosphatidylcholine and fatty acids prepared at pH 10 and then dialyzed to pH 7 (Wilschut et al., 1992). It is also possible that, in our nonphospholipid LUV system prepared at pH 9 and dialyzed to pH 7.4 or 6.0, a pH gradient was also established between the internal and external aqueous phases with some of the fatty acids moving preferentially toward the inner leaflet of the lipid bilayer where they can maintain their negative charge. Consequently, cholesterol sulfate, at a relatively small percentage, was present in the vesicles as the only other negatively charged group in the outer leaflet of the bilayer, rendering relatively unstable vesicles. At pH 6, the LUVs became even less stable because the pH was now approaching values below the pK_a of fatty acids in a membrane. In egg yolk phospholipid vesicles, 5-DSA EPR data indicated the coexistence of both ionized and nonionized forms of 5-DSA at pH 6.2 (Egret-Charlier et al., 1978). Interestingly, the effective diameter of our LUVs at pH 6 increased by only ~20% before precipitation was observed after 15 h. As the LUV systems at pH <9 remained stable for a short period of time, it may be possible to prepare and store LUVs at pH 9 and later to dialyze the samples to low pH values for molecular studies at pH <9. When this is done, QELS data should accompany the molecular studies to insure the integrity of the LUVs for quantitative interpretation of the data. For example, our QELS data showed that the LUVs at pH 6 were broadly distributed around 128 nm and remained stable for more than 15 but less than 24 h.

Fatty acid spin labels were used to monitor local dynamic properties of the lipid molecules in the bilayer. 5-DSA reports on motion near the polar headgroup region whereas 12-DSA describes motion in the center of the alkyl chain (Jost et al., 1971; Smith, 1972; Zhang and Fung, 1994). In phospholipid systems, it is generally accepted that the spin labels are randomly distributed between the two membrane bilayer leaflets, although the precise distribution is not clear. The nitroxide groups on the stearic acids are located near the lipid molecule head groups, and are closer to the membrane exterior than the analogous position of the phospholipid acyl chains (Ellena et al., 1988). Our results demonstrate that molecular motion near the polar headgroup was more restricted than the motion in the alkyl chain region in the center of the bilayer throughout the temperature range studied (25–90°C). Relatively smaller temperature-induced increases in motion were observed near the polar headgroup region than in the center of the alkyl chain. It is interesting to note that 12-DSA reported rapid changes in motion at ~60°C, a temperature cited as the "melting" of the alkyl chain by infrared and DSC data (Golden et al., 1987). Above 72°C, little motional change was observed in the alkyl chains upon increase in temperature. The motional properties of lipids in the bilayer depend on molecular packing and molecular interaction among lipid molecules. When an understanding of the distribution of different lipid molecules in the lipid leaflets is available, the local motional properties observed by either 5-DSA or 12-DSA can then be interpreted in more detail.

Our results showed that the partitioning of fatty acid derivative molecules (spin labels) between lipid and aqueous phases was temperature dependent and generally correlated with the phase transition observed by DSC and the alkyl chain mobility observed by EPR. However, large differences were observed between 5-DSA and 12-DSA molecules. At 25°C, when 5-DSA was introduced to the LUV system at pH 9 at a lipid-to-label ratio of 150, almost all of the 5-DSA was in the lipid phase and only ~1% of 5-DSA was in the aqueous phase, with a partition ratio (lipid/aqueous) of 96. However, ~74% of 12-DSA was in the lipid phase and 26% in the aqueous phase, with a partition ratio of ~3. Partitioning of 5-DSA into the aqueous phase increased upon temperature increase to ~5% to give a partition ratio of 23 at 90°C. In contrast, for 12-DSA, relatively small changes in the partitioning of 12-DSA were observed between 25 and 90°C. Among the small temperature-induced changes for 12-DSA, a minimum partition coefficient at ~40°C was observed. At this time, no molecular mechanism is obvious for explaining these phenomena. However, the differences observed between the partitioning of 5-DSA and 12-DSA in LUVs at pH 9 can be speculated. 5-DSA and 12-DSA are both derived from stearic acid, with the plane of the doxyl ring perpendicular to the long axis of the molecule (Broldo et al., 1982). Thus the only structural difference between these two molecules is the position of the doxyl spin label moiety, at C5 for 5-DSA and C12 for 12-DSA. This small structural difference produces different polarities for the two molecules. As van der Waals interactions are important in lipid alkyl chain packing, the location of the doxyl spin label on the alkyl chain is expected to affect the overall polarity and hydrophobicity of the molecules and thus affect the partitioning of the molecules in the bilayer. The difference in partitioning of 12-DSA and 5-DSA has also been noted for phospholipid vesicles (Sentjurc et al., 1990). It is also interesting to note that the melting point was 51–53°C for 5-DSA and 10–12°C

for 12-DSA (technical information from Aldridge Chem. Co., Milwaukee, WI). Our results suggested that in designing drug molecules with somewhat polar functional groups (for example, similar to that of the nitroxide moiety) to be in the stratum corneum lipid phase, it is desirable to attach the functional group to a fatty acid molecule close to the headgroup position to provide ~99% partitioning into the lipid phase.

In summary, we have used commercially available lipids to successfully prepare relatively stable and well characterized LUVs with lipid compositions and thermodynamic properties very similar to those in stratum corneum. We also demonstrated the time-dependent pH effects on the size and dispersity of the LUVs. Spin label EPR results indicated more restricted motion near the polar region than near the alkyl chain region. We also showed that the partitioning of 5-DSA and 12-DSA between LUV lipid and aqueous phases under similar conditions were quite different from each other. We believe that these results provide foundations for additional studies of stratum corneum LUVs with other molecules and/or of LUVs with different lipid composition leading to better understanding of the physical and functional properties of stratum corneum lipids.

We are most grateful to Dr. P. Walling of Helene Curtis and Dr. R. Harper of Hilltop Research, Inc. (Cincinnati, OH) for their initiation and support of this project. We thank Drs. C. Herb and T. Evans and Mr. K. Ikeda of Helene Curtis for their generous time and helpful discussions on QELS, DSC, and scanning densitometry analysis, respectively. We also thank Dr. W. Abraham of Cygnus Therapeutic Systems (Redwood City, CA) for discussions on methods of stratum corneum lipid vesicle preparation.

This work was supported by funds from Helene Curtis Industries, Inc. and Loyola University of Chicago.

REFERENCES

Abraham, W. 1992. Structures formed by epidermal lipids in vitro. *Sem. Dermatol.* 11:121–128.

Behrendt, H., and M. Green. 1971. Patterns of Skin pH from Birth through Adolescence. Charles C. Thomas, Springfield, IL.

Blank, I. H. 1952. Factors which influence the water content of the stratum corneum. *J. Invest. Dermatol.* 18:433–440.

Bleau, G., F. H. Bodley, J. Longpre, A. Chapdelaine, and K. D. Roberts. 1974. Cholesterol sulfate. I. Occurrence and possible biological function as an amphipathic lipid in the membrane of the human erythrocyte. *Biochim. Biophys. Acta.* 352:1–9.

Blume, A., M. Jansen, M. Ghyczy, and J. Gareiss. 1993. Interaction of phospholipid liposomes with lipid model mixtures for stratum corneum lipids. *Int. J. Pharm.* 99:219–228.

Braun-Falco, O., and H. C. Korting. 1986. Der normale pH-Wert der menschlichen Haut. *Hautarzt.* 37:126–129.

Broldo, M. S., I. Belsky, and E. Melrovitch. 1982. Comparative study of the esr behavior of doxyl-labeled and azethoxyl-labeled fatty acids in several liquid crystalline mesophases. *J. Phys. Chem.* 86:4197–4205.

Brown, L. R., C. Bösch, and K. Wüthrich. 1981. Location and orientation relative to the micelle surface for glucagon in mixed micelles with dodecylphosphocholine: EPR and NMR studies. *Biochim. Biophys. Acta.* 642:296–312.

Downing, D. T. 1992. Lipid and protein structures in the permeability barrier of mammalian epidermis. *J. Lipid Res.* 33:301–313.

Downing, D. T., W. Abraham, B. K. Wegners, K. M. William, and J. L. Marshall. 1993. Partitioning of sodium dodecyl sulfate into stratum corneum lipid liposomes. *Arch. Dermatol. Res.* 285:151–157.

Eastman, S., J. Wilschut, P. R. Cullis, and M. J. Hope. 1989. Intervesicular exchange of lipids with weak acid and weak base characteristics: influence of transmembrane pH gradients. *Biochim. Biophys. Acta.* 981:178–184.

Egret-Charlier, M., A. Sanson, and M. Ptak. 1978. Ionization of fatty acids at the lipid-water interface. *FEBS Lett.* 89:313–316.

Elias, P. M., and D. Friend. 1975. The permeability barrier in mammalian epidermis. *J. Cell. Biol.* 65:180–191.

Ellena, J., S. Archer, R. Dominey, B. Hill, and D. Cafiso. 1988. Localizing the nitroxide group of fatty acid and voltage-sensitive spin labels in phospholipid bilayers. *Biochim. Biophys. Acta.* 940:63–70.

Freed, J. H. 1976. Theory of slow tumbling EPR spectra for nitroxides. *In* Spin Labeling: Theory and Applications. L. J. Berliner, editor. Academic Press, New York. 53–132.

Friberg, S. E., and D. W. Osborne. 1985. Small angle x-ray diffraction patterns of stratum corneum and a model structure for its lipids. *J. Dispers. Sci. Tech.* 6:485–495.

Fung, L. W.-M., and M. E. Johnson. 1983. Temperature dependence of spin-label intensity in solutions and its implication in spin-labeled erythrocyte membrane studies. *Biophys. J.* 43:255–257.

Fung, L. W.-M., and M. E. Johnson. 1984. Recent developments in spin label EPR methodology for biomembrane studies. *In* Current Topics in Bioenergetics. P. Lee, editor. Academic Press, New York. 107–157.

Fung, L. W.-M., and Y. Zhang. 1990. A method to evaluate the antioxidant system for radicals in erythrocyte membranes. *Free Rad. Biol. Med.* 9:289–298.

Golden, G. M., D. B. Guzek, R. R. Harris, J. E. McKie, and R. O. Potts. 1986. Lipid thermotropic transitions in human stratum corneum. *J. Invest. Dermatol.* 86:255–259.

Golden, G. M., D. B. Guzek, A. H. Kennedy, J. E. McKie, and R. O. Potts. 1987. Stratum corneum lipid phase transitions and water barrier properties. *Biochemistry.* 26:2382–2388.

Gray, G. M., and R. J. White. 1979. Epidermal lipid liposomes: a novel non-phospholipid membrane system. *Biochem. Soc. Trans.* 7:1129–1131.

Gray, G. M., R. J. White, R. H. Williams, and H. J. Yardley. 1982. Lipid composition of the superficial stratum corneum cells of the epidermis. *Br. J. Dermatol.* 106:59–63.

Griffith, O. H., P. J. Dehlinger, and S. P. Van. 1974. Shape of the hydrophobic barrier of phospholipid bilayers (evidence for water penetration in biological membranes). *J. Membr. Biol.* 15:159–192.

Griffith, O. H., and P. C. Jost. 1976. Lipid spin labels in biological membranes. *In* Spin Labeling: Theory and Applications. L. J. Berliner, editor. Academic Press, New York. 453–523.

Hadgraft, J., K. A. Walters, and R. H. Guy. 1992. Epidermal lipids and topical drug delivery. *Sem. Dermatol.* 11:139–144.

Hope, M. J., M. B. Bally, G. Webb, and P. R. Cullis. 1985. Production of large unilamellar vesicles by a rapid extrusion procedure: characterization of size distribution, trapped volume and ability to maintain a membrane potential. *Biochim. Biophys. Acta.* 812:55–65.

Hope, M. J., and P. R. Cullis. 1987. Lipid asymmetry induced by transmembrane pH gradients in large unilamellar vesicles. *J. Biol. Chem.* 262: 4360–4366.

Hou, S. Y. E., S. J. Rehfeld, and W. Z. Plachy. 1991. X-ray diffraction and electron paramagnetic resonance spectroscopy of mammalian stratum corneum lipid domains. *Adv. Lipid Res.* 24:141–171.

Johnson, M. E. 1979. Spin-label techniques for monitoring macromolecular rotational motion: empirical calibration under nonideal conditions. *Biochemistry.* 18:378–384.

Jost, P., L. J. Libertini, V. C. Herbert, and O. H. Griffith. 1971. Lipid spin labels in lecithin multilayers: a study of motion along fatty acid chains. *J. Mol. Biol.* 59:77–98.

Kim, Y.-H., W. I. Higuchi, J. N. Herron, and W. Abraham. 1993a. Flourescence anisotropy studies on the interaction of the short chain n-alkanols with stratum corneum lipid liposomes (SCLL) and distearoylphosphatidylcholine (DSPC)/distearoylphosphatidic acid (DSPA) liposomes. *Biochim. Biophys. Acta.* 1148:139–151.

Kim, C.-K., M.-S. Hong, Y.-B. Kim, and S.-K. Han. 1993b. Effects of penetration enhancers (pyrrolidone derivatives) on multilamellar liposomes of stratum corneum lipid: A study by UV spectroscopy and differential scanning calorimetry. *Int. J. Pharm.* 95:43–50.

Kitagawa, S., M. Sawada, and H. Hirata. 1993. Fluorescence analysis with diphenylhexatriene and its ionic derivatives of the fluidity of liposomes

constituted from, stratum corneum lipids: contribution of each lipid component and effects of long-chain unsaturated fatty acids. *Int. J. Pharm.* 98:203–208.

Kitson, N., M. Monek, K. Wong, J. Thewalt, and P. Cullis. 1992. The influence of cholesterol 3-sulphate on phase behavior and hydrocarbon order in model membrane systems. *Biochim. Biophys. Acta.* 1111:127–133.

Kitson, N., J. Thewalt, M. Lafleur, and M. Bloom. 1994. A model membrane approach to the epidermal permeability barrier. *Biochemistry.* 33: 6707–6715.

Kittayanond, D., C. Ramachandran, and N. Weiner. 1992. Development of a model of the lipid constituent phase of the stratum corneum. I. Preparation and characterization of "skin lipid" liposomes using synthetic lipids. *J. Soc. Cosmet. Chem.* 43:149–160.

Klösgen, B., and W. Helfrich. 1993. Special features of phosphatidylcholine vesicles as seen in cryo-transmission electron microscopy. *Eur. Biophys. J.* 22:329–340.

Lasic, D. D. 1992. Liposomes. *Am. Sci.* 80:20–31.

Madison, K. C., D. C. Swartzendruber, P. W. Wertz, and D. T. Downing. 1987. Presence of intact intercellular lamellae in the upper layers of the stratum corneum. *J. Invest. Dermatol.* 88:714–718.

Marsh, D. 1982. Electron spin resonance: spin label probes. *In* Techniques in Life Sciences (Lipid and Membrane Biochemistry-Part II). B4/II, B426:1–44.

Mattai, J., C. L. Froebe, L. D. Rhein, F. A. Simion, H. Ohlmeyer, D. T. Su, and S. E. Friberg. 1993. Prevention of model stratum corneum lipid phase transitions in vitro by cosmetic additives: differential scanning calorimetry, optical microscopy, and water evaporation studies. *J. Soc. Cosmet. Chem.* 44:89–100.

Mayer, L. D., M. J. Hope, P. R. Cullis, and A. S. Janoff. 1985. Solute distribution and trapping efficiencies observed in freeze-thawed multilamellar vesicles. *Biochim. Biophys. Acta.* 817:193–196.

Melnik, B. C., J. Hollmann, E. Erler, B. Verhoeven, and G. Plewig. 1989.Microanalytical screening of all major stratum corneum lipids by sequential high-performance thin-layer chromatography. *J. Invest. Dermatol.* 92:231–234.

Miyazaki, J., H. Kalman, and D. Marsh. 1992. Interfacial ionization and partitioning of membrane-bound local anaesthetics. *Biochim. Biophys. Acta.* 1108:62–68.

Onken, H. D., and C. A. Moyer. 1963. The water barrier in human epidermis. *Arch. Dermatol.* 87:584–590.

Ptak, M., M. Egret-Charlier, A. Sanson, and O. Bouloussa. 1980. A NMR study of the ionization of fatty acids, fatty amines and *N*-acyl amino acids incorporated into phosphatidylcholine vesicles. *Biochim. Biophys. Acta.* 600:387–397.

Scheuplein, R. J., and I. H. Blank. 1971. Permeability of the skin. *Physiol. Rev.* 51:702–747.

Sentjurc, M., G. Bacic, and H. M. Swartz. 1990. Reduction of doxyl stearates by ascorbate in unilamellar liposomes. *Arch. Biochem. Biophys.* 282:207–213.

Smith, I. C. P. 1972. The spin label method. *In* Biological Applications of Electron Spin Resonance. H. M. Swartz, J. R. Bolton, and D. C. Borg, editors. Wiley Interscience, New York. 483–539.

Szoka, F. C. 1987. Lipid vesicles. Model systems to study membrane-membrane destabilization and fusion. *In* Cell Fusion. A. E. Sowers, editor. Plenum Press, New York. 209–240.

Wertz, P. W., W. Abraham, L. Landmann, and D. T. Downing. 1986. Preparation of liposomes from stratum corneum lipids. *J. Invest. Dermatol.* 87:582–584.

Wertz, P. W., D. C. Swartzendruber, K. C. Madison, and D. T. Downing. 1987. Composition and morphology of epidermal cyst lipids. *J. Invest. Dermatol.* 89:419–425.

White, S. H., D. Mirejovsky, and G. I. King. 1988. Structure of lamellar lipid domains and corneocyte envelopes of murine stratum corneum: an x-ray diffraction study. *Biochemistry.* 27:3725–3732.

Williams, A. C., and B. W. Barry. 1992. Skin absorption enhancers. *Crit. Rev. Ther. Drug Carrier Sys.* 9:305–353.

Williams, M. L., and P. M. Elias. 1981. Stratum corneum lipids in disorders of cornification. I. Increased cholesterol sulfate content of stratum corneum in recessive x-linked ichthyosis. *J. Clin. Invest.* 68:1404–1410.

Wilschut, J., J. Scholma, S. J. Eastman, M. J. Hope, and P. R. Cullis. 1992. Ca^{2+}-induced fusion of phospholipid vesicles containing free fatty acids: modulation by transmembrane pH gradients. *Biochemistry.* 31:2629–2636.

Winterhalter, M., and D. D. Lasic. 1993. Liposome stability and formation: experimental parameters and theories on the size distribution. *Chem. Phys. Lipids.* 64:35–43.

Zhang, Y., and L. W.-M. Fung. 1994. The roles of ascorbic acid and other antioxidants in the erythrocyte in reducing membrane nitroxide radicals. *Free Rad. Biol. Med.* 16:215–222.